

pubs.acs.org/synthbio Research Article

Emergent Damped Oscillation Induced by Nutrient-Modulating Growth Feedback

Juan Melendez-Alvarez, Changhan He, Rong Zhang,* Yang Kuang, and Xiao-Jun Tian*



Cite This: ACS Synth. Biol. 2021, 10, 1227-1236



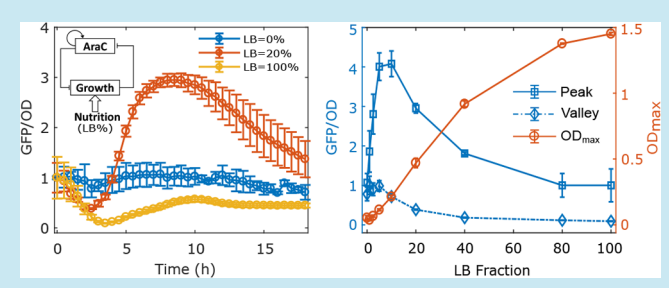
ACCESS

Metrics & More

Article Recommendations

Supporting Information

ABSTRACT: Growth feedback, the inherent coupling between the synthetic gene circuit and the host cell growth, could significantly change the circuit behaviors. Previously, a diverse array of emergent behaviors, such as growth bistability, enhanced ultrasensitivity, and topology-dependent memory loss, were reported to be induced by growth feedback. However, the influence of the growth feedback on the circuit functions remains underexplored. Here, we reported an unexpected damped oscillatory behavior of a self-activation gene circuit induced by nutrient-modulating growth feedback. Specifically, after dilution of



the activated self-activation switch into the fresh medium with moderate nutrients, its gene expression first decreases as the cell grows and then shows a significant overshoot before it reaches the steady state, leading to damped oscillation dynamics. Fitting the data with a coarse-grained model suggests a nonmonotonic growth-rate regulation on gene production rate. The underlying mechanism of the oscillation was demonstrated by a molecular mathematical model, which includes the ribosome allocation toward gene production, cell growth, and cell maintenance. Interestingly, the model predicted a counterintuitive dependence of oscillation amplitude on the nutrition level, where the highest peak was found in the medium with moderate nutrients, but was not observed in rich nutrients. We experimentally verified this prediction by tuning the nutrient level in the culture medium. We did not observe significant oscillatory behavior for the toggle switch, suggesting that the emergence of damped oscillatory behavior depends on circuit network topology. Our results demonstrated a new nonlinear emergent behavior mediated by growth feedback, which depends on the ribosome allocation between gene circuit and cell growth.

KEYWORDS: circuit—host interactions, metabolic burden, ribosome, resource allocation, topology

Rational design and forward engineering of synthetic gene circuits based on general principles have demonstrated its power in successfully constructing, testing, and debugging circuits for many remarkable applications in the past. However, the complex interplay between the gene circuit and the host cell physiology at various scales often makes the circuit functions fragile to the environmental fluctuations.⁵⁻¹¹ The transcription and translation of heterologous gene circuits steal a considerable amount of the host cell's resources that are originally allocated for host activities, thus inevitably leading a significant metabolic burden to the host cell. 12-15 The altered physiology to host cells, in turn, affects the circuit intended function. $^{16-20}$ Furthermore, the host environmental fluctuations make the circuit-host interplay more complicated and make circuit behavior hard to predict. Thus, it is essential to understand the general principle of how these circuit-host interactions affect the functionality and consider these substantial effects into the design of gene circuits.

One of the most important circuit—host interactions is the growth feedback, in which circuit gene expression slowdowns the host cell growth while the host cell growth also affects the circuit gene expression. ^{19,21–24} Previous studies have reported various emergent circuit properties that result from growth

feedback. For example, growth feedback could increase the ultrasensitivity of the gene circuit and thus make a non-cooperative positive autoregulatory system bistable. ²⁴ On the other hand, the growth feedback could also drastically alter circuit functions. Recently, we found a topology-dependent interference of synthetic gene circuit function by growth feedback. ¹⁹ We tested two synthetic memory circuits, self-activation switch and toggle switch, and found that both circuits interact with host cells through growth feedback but behave differently. While the self-activation switch quickly lost its memory due to the fast dilution of circuit products mediated by host cell growth, the toggle switch is more robust to the growth feedback and retains its memory after the fast growth phase. It is also reported that an increase of nutrients may lead to a bistable switch circuit transition from bistability

Received: January 28, 2021 Published: April 29, 2021





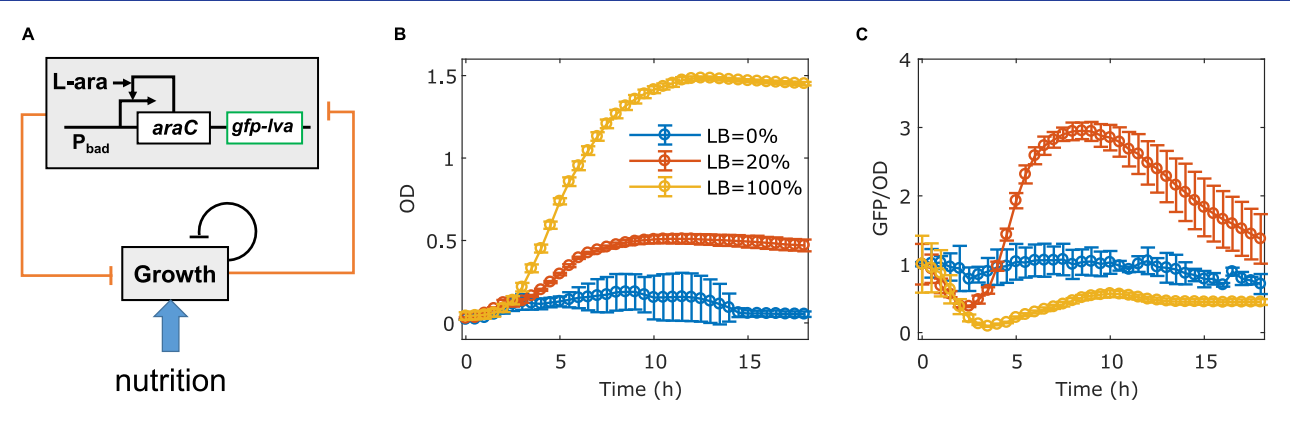


Figure 1. Unexpected oscillatory dynamics induced by growth feedback with varied nutrition level in the SA circuit. (A) Diagram of interactions between the self-activation (SA) gene circuit and the host cell growth, which is modulated by the nutrient. In the SA circuit, transcriptional factor AraC forms a dimer and binds to promoter P_{BAD} in the presence of stimulus L-(+)-arabinose (L-ara), and thus activates the expression of itself. Unstable GFP variant (GFP-lva) is used as the reporter. (B,C) Dynamics of growth (Optical Density, OD) (B) and GFP/OD (C) after 1:100 dilution of cells with activated SA circuit into fresh medium with a high dose of L-ara and three nutrient levels with 0%, 20%, and 100% LB in the culture medium. The data with 100% LB and 0% LB are from a previous work. Data indicate mean \pm s.d. (n = 4).

to monostability.²⁵ However, the influence of the circuit dynamics by the growth feedback remains underexplored.

Here we studied how the growth feedback and its effects on gene circuits are modulated by nutrient level. Followed by our previous work, 19 we diluted the cells with an activated selfactivation switch into the fresh medium with reduced nutrition level with a high dose of inducer L-ara. It is surprising to us that the circuit expression level showed very unexpected damped oscillatory dynamics in a broad range of nutrition levels. Specifically, after dilution into the fresh medium with moderate nutrients, the circuit gene expression first decreases as the cell grows and then shows a significant overshoot before it reaches the steady state. To understand the mechanism of this unexpected phenomenon at the coarse-grained level, we revised our previous model by considering the regulation of the circuit production rate by growth rate. Fitting this model to the experimental data suggests that the production rate could nonmonotically depend on the growth rate. To further understand the mechanism at the molecular level, we built another model by including the ribosome allocation toward gene production, cell growth, and cell maintenance. Interestingly, our model predicted that the oscillation amplitude shows a nonmonotonic relation with respect to the nutrient level, where the highest peak was found in the medium with moderate but not rich nutrients. We experimentally verified this prediction by tuning the nutrient level with various LB fractions in the culture medium. In addition, the emergence of oscillatory behavior depends on circuit network topology, as we did not observe significant oscillatory behavior for the toggle switch.

RESULTS AND DISCUSSION

Unexpected Oscillatory Dynamics Induced by Growth Feedback with Varied Nutrition Level. In our previous work, 19 we built a simple synthetic self-activation (SA) gene circuit (Figure 1A), in which the transcription factor AraC activates the expression of itself by binding to its promoter $P_{\rm BAD}$. Reporter gene green fluorescent protein (GFP) was used to visualize the dynamics of AraC. The design is similar to the previously reported positive feedback synthetic gene circuit. We expected that this circuit behaves as bistable switch. However, we found that the circuit did not exhibit hysteresis even as a stable bimodal distribution was observed. 19

The underlying reason is that the gene circuits interact with the host cell growth (Figure 1A), which led to the loss of memory for the self-activation circuit after diluting the activated cells into the fresh 100% Lysogeny broth (LB) rich medium. The memory can be maintained well with the M9 minimal culture low-nutrient (0% LB) medium. Here in this work, we studied how the nutrient level modulates the growth feedback and circuit dynamics (Figure 1A).

We first varied nutrition levels by mixing 20% of LB media and 80% of M9 media where there is no cell growth. We measured the temporal dynamics of the cell growth and circuit gene expression after diluting the activated cell into a fresh medium with 20% LB and a high/low dose of circuit inducer Lara. We observed that the cell growth followed the logistic model in both moderate and rich nutrient mediums, with a smaller population carrying capacity in the 20% LB medium (Figure S1A, Figure 1B). Consistent with our previous work by diluting cells into the fresh medium with 100% LB and a low dose of L-ara, the circuit memory is also lost due to the high division rate in the medium with 20% LB (Figure S1B). This result confirmed that the SA circuit is susceptible to growth feedback, even with moderate nutrients in the growth medium. In the medium with high L-ara, the average GFP level (GFP/ OD) decreases through the log-phase until it reaches a minimum, consistent with 100% LB medium (Figure 1C). However, the circuit dynamics changed dramatically with moderate nutrients after the valley. The GFP level exhibits significant overshoot behavior before the system settles down to the steady state, instead of reaching the steady state directly as in the 100% LB medium. It is noted that here the maximum OD is about 0.5 in the 20% LB medium, so no calibration was needed to calculate GFP/OD.²⁷ This unexpected damped oscillation phenomenon suggests that the nutrient could significantly alter the growth feedback and the synthetic gene circuit dynamics.

Theoretical Analysis Suggests a Nonmonotonic Growth-Rate Regulation on Gene Production Rate. To understand the underlying mechanism of the emergent oscillatory behavior induced by growth feedback with a varied nutrition level, we first tested the simplified coarse-grained model from our previous work. ¹⁹ We found that the model is not able to fit the data well. This is consistent with our theoretical proof that there is no overshoot with this simplified

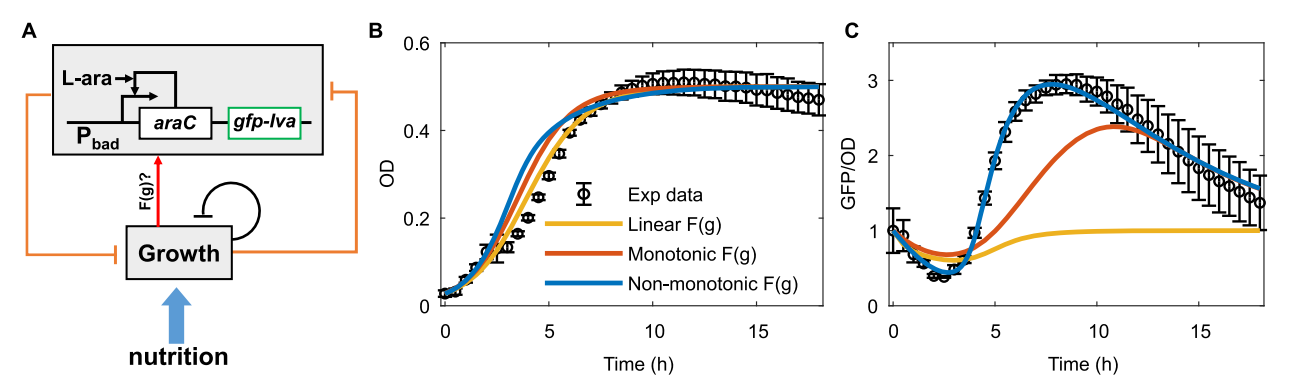


Figure 2. Theoretical analysis suggests a nonmonotonic growth-rate regulation on gene production rate. (A) The diagram of the model by considering the regulation of the production rate of the SA circuit by growth rate. (B,C) Fitting of the model to the dynamics of the host cell growth (B) and the circuit gene expression (C). Linear (yellow lines), monotonic (orange lines), and nonmonotonic (blue lines) functions were used to test the regulation of the production rate of the gene circuit by growth rate (F(g)) and only the nonmonotonic function enables the models to fit the experimental data perfectly.

model (see Supporting Information, Proposition 1). This simplified model included the growth-mediated dilution but did not consider potential regulations of gene production by growth rate. This model was able to explain the memory loss of the SA circuit after diluting into a fresh medium with rich nutrients where the growth-mediated dilution plays the dominant role, as demonstrated previously.¹⁹

Here the overshoot behavior from the varied nutrient level strongly suggests that host cell growth could increase the production rate of synthetic gene circuits. Thus, we revised the model by adding a growth rate-dependent function F(g) on the circuit gene production rate (Figure 2A, see the Methods for details). We used several different functions to test the monotonicity of F(g). We found that both a monotonous function and a linear function of F(g) are not able to fit the data well (Figure 2B,C, red/yellow lines). We further proved that when F(g) is a monotonously decreasing function or positive linear function, there is no overshoot (see Supporting Information, Proposition 2 and 3). It is noted that in the monotonous scenario, imperfectly fitted oscillation is found. The underlying reason is that the function of production rate on growth rate F(g) is almost saturated for a long time period (0-10 h) even the growth rate decreased significantly to a very low level at 5 h (Figure S2A), which is from the extremely low threshold for the saturation of F(g) on growth rate (Figure S2A). Thus, in the early phase, the dilution dominates, leading to the decrease of GFP, while in the middle phase, the dilution is reduced due to decreased growth rate but the production rate is not yet decreased much due to the saturation, leading to a small overshoot. However, the model with monotonic dependence under this extreme condition is still not able to fit the experimental data well.

We then used a nonmonotonic function of F(g) and found that it fits the data satisfactorily (Figure 2B,C, blue lines). The fitting result shows that F(g) first decreases a bit and then increased with time quickly to a peak and then decreases to the basal level (Figure S2C). The analysis suggests that F(g) first increases and then decreases with growth rate (Figure S2D). In the early fast growth stage, the reduced production rate and immediate dilution because of fast growth lead to a sharp GFP decrease. As the cell growth slows down, an increase of the production rate mediated by growth overcomes the reduced dilution, leading to the increase and overshoot of GFP. Finally, in the stationary phase, GFP relaxes to the steady state where

growth ceases. Taken together, our theoretical analysis suggests that there is a nonmonotonic growth-rate regulation on gene production rate, which accounts for the emergence of the damped oscillation behavior.

Molecular Mechanism for the Growth Rate Regulation on Gene Production Rate. The regulation of the circuit gene production rate by growth rate is largely dependent on the fact that the ribosome level in the host cell increases with growth rate. To further understand the oscillatory behavior at the molecular level, we also developed a mathematical model by integrating the ribosome dynamics and its allocation to the circuit gene production and gene expression for the host cell growth (Figure 3A) (see Methods for details). Basically, the ribosome level increases with the growth rate *via* an autocatalysis way. The allocation of ribosome to host cell growth and synthetic gene expression depends on the compromised growth rate and resource demands.

Upon data fitting, this model successfully captured the oscillatory dynamics of the circuit gene expression (Figure 3B,C). The ribosome is increased quickly after the dilution but is mainly allocated to cell growth at the early stage (Figure 3D, blue and red lines). The allocated ribosome to the circuit is limited at this stage (Figure 3D, yellow line), and thus the production of the gene circuit is kept at a low level (Figure 3E, blue line). The limited ribosome to the circuit and the dilution from the fast growth make the GFP level decrease quickly. When the cell growth becomes slower, the ribosome level has accumulated and continues to increase due to the autocatalysis (Figure 3D, blue line), but the ribosome demand from the cell growth starts to decrease (Figure 3D, red line), thus leading to the spare ribosome allocated to the gene circuit (Figure 3D, blue line), a fast increase of the production rate of the circuit gene expression (Figure 3D, yellow line), and the overshoot of GFP level to a very high level. When the ribosome decreases to the low level at the stationary phase, the GFP level also reaches the steady-state. The fold change of ribosome allocated to the synthetic circuit and the growth rate follows a nonmonotonic correlation (Figure 3F, red curve), similar to the nonmonotonic regulation function of gene circuit production rate by growth rate (Figure 3F, blue curve, Figure S2D). It is noted that here the effect of growth rate on the production rate is not immediate like the coarse-grained model. The accumulation of ribosome causes some delay for the growth

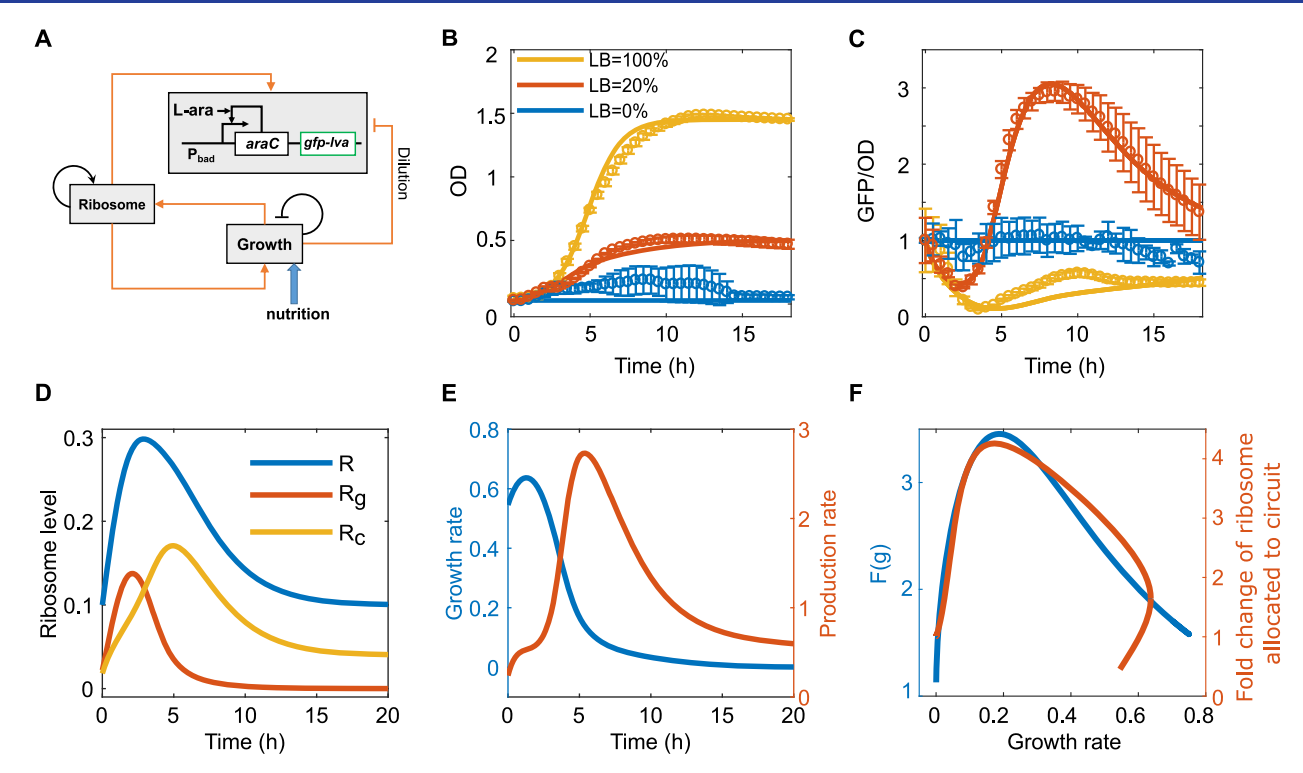


Figure 3. Molecular mechanism for the growth rate regulation on gene production rate. (A) The diagram of the model by considering the ribosome regulation and allocation. (B,C) Fitting of the model to the dynamics of the host cell growth (B) and circuit gene expression (C). Solid lines are model simulation, and the dotted lines with error bars are experimental data. The data with 100% LB and 0% LB shown here as control. (D) The temporal dynamics of the ribosome production and allocation to the cell growth and the SA circuit. (E) The temporal dynamics of the growth rate and production rate of the synthetic gene circuit. (F) The nonmonotonic regulation function of gene circuit production rate by growth rate (F(g), blue curve) in the coarse-grained model and the fold change of ribosome allocated to the synthetic circuit (R_{cp} red line) in the ribosome model as a function of growth rate.

rate to reach a maximum value. Thus, the ribosome allocation to the circuit and growth are different before and after the maximum growth rate, and their correlation curve shows two values around the maximum growth rate. Thus, the model not only provides a molecular mechanism for the emergent damped oscillation induced by growth feedback but also for nonmonotonic growth-rate regulation on gene production rate.

The Amplitudes of the Oscillatory Dynamics Are Controlled by Nutrient Level. Figure 1 suggested that the damped oscillation emerged in some range of nutrient level but vanished after one nutrient threshold. To systematically study how the oscillatory behavior depends on the nutrient level, we analyzed the dynamics of the circuit gene expression by varying one parameter, carrying capacity $(N_{\rm max})$, in the model. $N_{\rm max}$ is a good indicator of nutrient level, given that the cell density reaches a different carrying capacity according to the nutrient level. ²⁹ It is noted that even $N_{\rm max}$ is not proportional to nutrient level; the positive dependence of $N_{\rm max}$ on the nutrient level could still give us a qualitative prediction about how the behavior emerged and vanished with the nutrient levels.

Figure 4A shows the model prediction about the dynamics of the circuit gene by varying $N_{\rm max}$ systematically. It is clear that the circuit gene expression always decreases immediately after dilution into the fresh medium to a valley (Figure 4A), and the depth of the valley increases with $N_{\rm max}$ (Figure 4B). This is reasonable given that the larger $N_{\rm max}$ gives a longer period of fast growth and thus the more dilution of the circuit gene expression, consistent with our previous work. After reaching the valley, the system starts to bounce back to the steady state with an overshoot and shows a distinct oscillatory

behavior for N_{max} < 1.15, or directly relaxes to the steady state without overshoot and shows an adaptation behavior if N_{max} > 1.15. That is, the damped oscillation can emerge with moderate nutrient levels but vanishes with rich nutrients. Interestingly, the oscillation peak first increases to a maximum at $N_{\rm max}$ = 0.379, and then decreases with $N_{\rm max}$ until converging with the steady state (Figure 4B). The transition from the damped oscillation to the adaptation largely depends on ribosome allocation and the gene activity at the valley points. Large N_{max} creates a long period of fast growth, which dilutes the circuit gene expression significantly and makes more ribosome allocated to cell growth (Figure S3A-C). Furthermore, for large $N_{\rm max}$ at the valley point, the low level of AraC leads to a very weak production of gene circuit due to its self-activation topology (Figure S3D). Thus, the circuit is not able to take advantage of the spared ribosome for overshooting before the system reaches a steady state (Figure

To verify this prediction experimentally, we tuned the nutrient level by varying the LB fraction in the culture medium from 0 to 100%. After dilution of the cells into the fresh medium, the host cell growth followed the logistic model to reach different carrying capacity according to the fraction of LB in the culture medium (Figure S4). The GFP dynamics with various LB fractions is shown in Figure 4C. A general decrease of GFP immediately after the dilution was observed for all the nutrient levels, and the overshoot was found in a broad nutrient range from 1% to 40% LB. Most importantly, Figure 4D shows that the valley depth increases with nutrient level and the maximum peak was found in the moderate medium

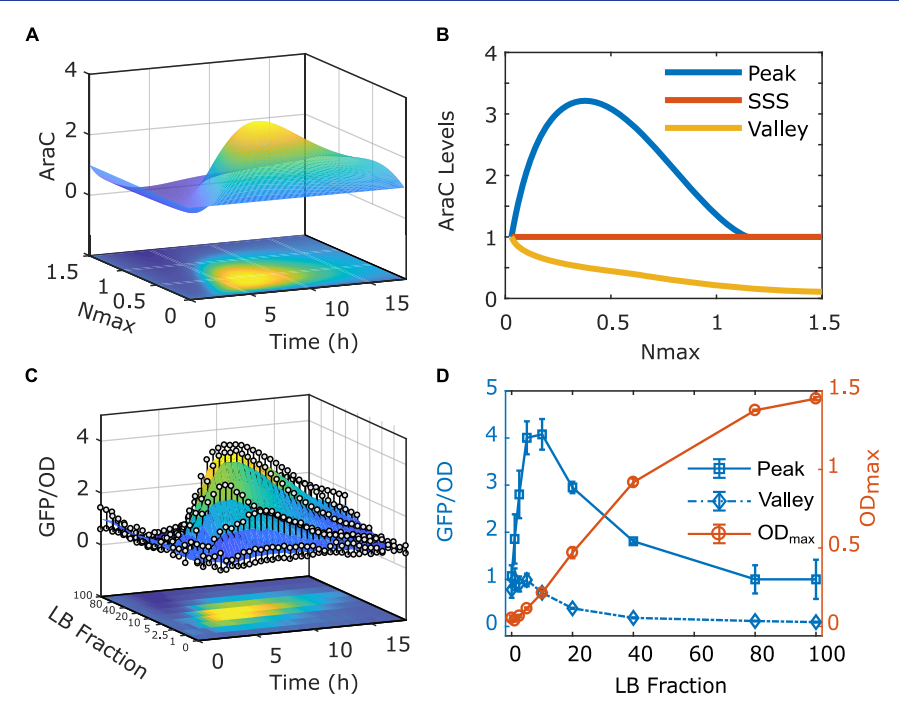


Figure 4. Amplitudes of the oscillatory dynamics in the SA circuit are controlled by nutrient level. (A,B) Model prediction about the dynamics of gene expression level (A) and the amplitudes of the oscillations (B) with various carrying capacity (N_{max}) in the SA circuit. (C) Dynamics of GFP/OD after 1:100 dilution of cells with activated SA switch into the fresh medium with various LB fractions. (D) The dependence of GFP/OD peak, valley, and maximum carrying capacity (OD_{max}) on the LB fraction in the culture medium. Data indicate mean \pm s.d. (n = 4).

(10% LB). Overshoot was not found in the medium with 80% and 100% LB, where the GFP level was relaxed to the steady state after the valley point. The dependence of carrying capacity $(N_{\rm max})$ on the LB fraction shown in Figure 4D confirmed that the $N_{\rm max}$ is a good indicator of the nutrient level in the theoretical analysis in Figure 4AB. It is noted that in the majority LB range (\leq 20% LB) of damped oscillation, the maximum OD is no larger than 0.5, and there is no need for calibration to calculate GFP/OD.²⁷ The oscillation peak in the medium with 40% LB could be smaller after calibration given that GFP/OD might be reported larger than the true values in the range of large OD because the calibrated OD could be larger than the reported OD. Thus, we experimentally validated our model prediction.

The Emergence of Oscillatory Behavior Depends on Circuit Network Topology. We further investigated whether the damped oscillation also emerges in other gene circuits. First, we tested a circuit without self-activation. We used a circuit in which the self-activation of the SA circuit was removed (Figure S5A). Interestingly, we found a similar damped oscillation (Figure S5B). It is noted that the oscillation peaks are not as high as the SA circuit, which is largely due to the self-activating nature of the latter. To further verify the topology dependence, we also measured the behavior of the toggle switch, which is another well-characterized bistable circuit with two genes (LacI and TetR) repressing the expression of each other (Figure 5A). In our previous work, we compared the SA switch and the toggle switch circuits in response to growth feedback. We found that the SA circuit was very sensitive to the growth-mediated dilution and lost its memory very easily, while the toggle switch was more refractory to the growth feedback and retrieved its memory after the fast-growth phase. 19 Here we tested whether the toggle switch circuit behaves differently in response to the nutrient-modulating growth feedback.

We applied the same modeling framework to the toggle switch (Figure 5A, and Methods for details). We did a theoretical analysis on the dynamics of the toggle switch after dilution of the host cells into the fresh medium by varying the carrying capacity N_{max} . We found that the LacI level dropped quickly to different levels according to the $N_{\rm max}$ values (Figure 5B). It is noted that the LacI level at the valley point decreases with N_{max} (Figure 5B), similar to the SA circuit (Figure 4A). This is reasonable because larger N_{max} ensures a longer duration of fast-growth phase and thus longer dilutiondominated phase. Interestingly, we did not observe a significant overshoot for the toggle switch (Figure 5B), which is different from the SA circuit. To illustrate the underlying mechanism, we analyzed the simulated trajectories (Figure 5C inset) in the direction field. As shown in Figure 5C, the system was initially in the LacI-high state (green circle) and then moved toward the LacI-low/TetR-low corner due to the dilution of both LacI and TetR in the fast-growth phase. Then, the system recovered back to its original state following the direction field without significant overshoot for all nutrient

Following the same experimental protocol to verify the prediction, we diluted the cells with an activated toggle switch into to fresh medium with different LB fractions. We found that after dilution the GFP level decreased to a minimum that depends on the LB fraction (Figure 5D), consistent with the model prediction. Furthermore, no significant overshoot was observed for all samples with various LB fractions (Figure 5D), which is also consistent with the model prediction. Thus, the emergence of oscillatory behavior depends on circuit network topology.

Here, we simply tuned the growth feedback by modulating the nutrient level with mixed LB and the M9 minimal culture media. In the future, it would be interesting to use a chemically defined medium with known chemical composition to fine-

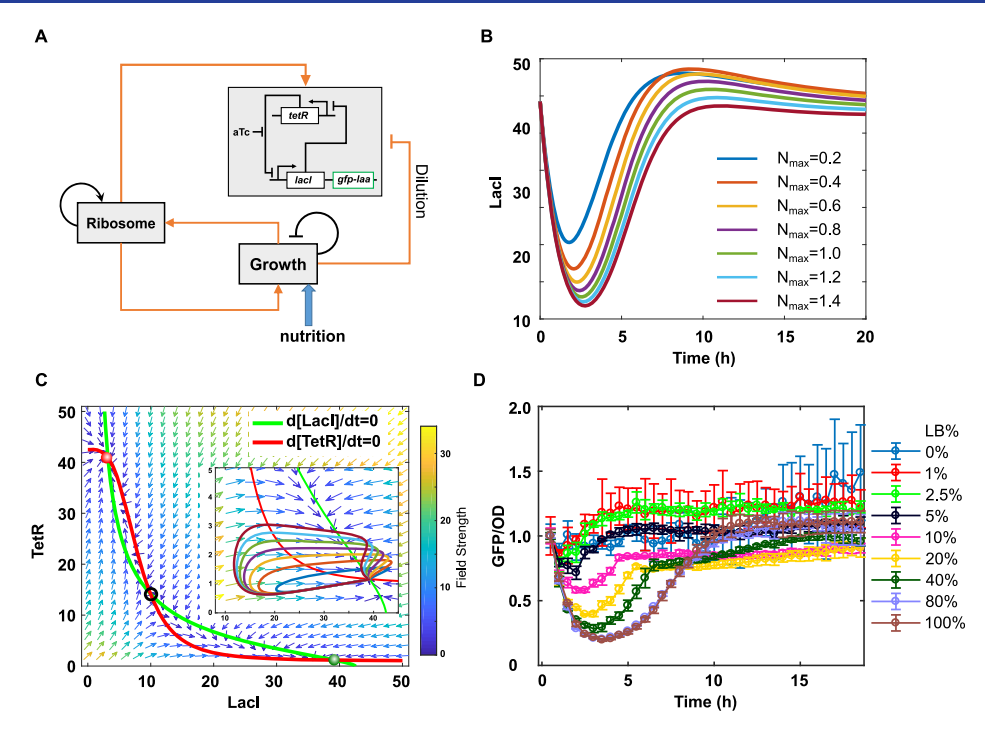


Figure 5. Emergence of oscillatory behavior depends on circuit network topology. (A) The diagram of the model for toggle switch circuit by considering the ribosome regulation and allocation. (B,C) Model prediction about the temporal dynamics of circuit gene expression level (B) and trajectories on the phase plane diagram (C) with various carrying capacity (N_{max}) . The nullclines of LacI and TetR are shown in green and red, respectively. The vector field of the system is represented by small arrows and the field strength is indicated by the color of the arrows. (D) Dynamics of GFP/OD after 1:100 dilution of cells with activated toggle switch into fresh medium with various LB fractions. Data indicate mean \pm s.d. (n=3).

tune the growth feedback and study its effects on gene circuits systematically. Recently, it is found that protein production strategies differ in response to starvation for carbon, nitrogen, or phosphate. On the strategies regulations under these nutrient limitations affect the growth feedback and the synthetic gene circuits. In addition, a fluctuating growth environment in different host cells and growth-feedback mediated metabolic toxicity affect the host cell metabolism and the circuit functions. Systematical measurement of the perturbed transcriptional/translational rates, growth rate, and the ribosome profiles at various phases of cell growth will significantly enhance our understanding of the modulation of growth feedback by nutrient levels and limits.

Understanding the growth feedback at the molecular level will greatly help us to formulate control strategies for engineering gene circuits robust to the host cell physiological environment. Here we considered the ribosome allocation in our mathematical model and found that the interaction between ribosome availability and growth condition due to different nutrient levels can produce unexpected outcomes in synthetic gene circuit dynamics. The competition of cellular resources between the endogenous genes and heterologous synthetic genes exist across multiple levels, including RNA polymerase (RNAP) at the transcriptional level and ClpXP at the protein turnover level, which are not considered here. Furthermore, it is unclear whether there is a priority for resource allocation. In addition, the consequences for the evolution is also very important. The loss of circuit functions can be regained through evolutionary mutations, which was demonstrated with one synthetic positive feedback gene circuit integrated into yeast cells.35

It is reported that guanosine tetraphosphate (ppGpp) plays a critical role in regulating bacterial growth, and ribosome regulation and allocation. Sophisticated regulations have been found on the regulations of ribosome and ppGpp, such as feedforward loop, positive feedback. Interestingly, ppGpp plays a central role in coordinating transcription and translation under nitrogen starvation, but is dispensable under carbon starvation. Integrating all of these orchestrators into one modeling framework will provide us a comprehensive understanding of growth feedback.

The effects of growth feedback on the gene circuits are diverse and depend on many factors. The effects could be beneficial and thus can be utilized to enhance the circuit functions, such as the increased ultrasensitivity.²⁴ The effects could also be detrimental, such as the loss of memory in the self-activation switch. 19 All these focused on the perturbation of the circuit steady-state behaviors by growth feedback. Here, we reported the unexpected alteration of the circuit dynamics by growth feedback. While the gene expression in the SA switch circuit shows emergent damped oscillation behavior with undershoot and overshoot around the steady state level, the gene expression in the toggle switch circuit only shows undershoot. This is further evidence that the toggle switch is more robust to growth feedback than the SA switch. Characterization of the general principles for the kinetic changes due to fluctuating growth conditions will facilitate our ability to utilize or minimize the effects of growth feedback.

METHODS AND MODELS

Strains, Media, Chemicals, and Plasmids. *E. coli* DH10B (Invitrogen, USA) was used for all the plasmid preparations. Measurement of the self-activated circuit was

performed in *E. coli* K-12 MG1655 Δ lacI Δ araCBAD, and measurement of the toggle switch was performed with *E. coli* K-12 MG1655 Δ lacI as described in the literature. ¹⁹ Inducers L-ara (L-(+)-Arabinose and aTc (Anhydrotetracycline hydrochloride, Abcam) were dissolved in ddH₂O at concentrations of 25% and 1 mg/mL, and stored at -20 °C in aliquots as stocking solutions. The aTc stocking solutions were replaced every month. When diluted into appropriate working solutions in ddH2O, L-ara solutions were replaced monthly, and aTc solutions were prepared freshly each time and discarded after 24 h. All the working solutions were kept at 4 °C and added into culture media with 1000-fold dilution. Details of the self-activated circuit and toggle switch can be found in the literature. ¹⁹

Culture Media. Before the cells were transferred into varied nutrient culture media they were cultured with LB broth (Luria—Bertani broth, Sigma-Aldrich) supplemented with 25 μ g/mL chloramphenicol or 50 μ g/mL kanamycin depending on the backbone of the circuit. The composition of LB broth is 10 g/L of NaCl, 10 g/L of tryptone and 5 g/L of yeast extract. The M9 minimal salts used to make varied nutrient culture media was purchased for Sigma-Aldrich, and the composition is 15 g/L of KH₂PO₄, 2.5 g/L of NaCl, 33.9 g/L of Na₂HPO₄, and 5 g/L of NH₄Cl.

Circuit Inductions. The experimental procedure for each biological replicate of the self-activated circuit (SA circuit) induction was carried out like this. On day one, SA circuit plasmid was transformed into E. coli strain K-12 MG1655∆lacI Δ araCBAD, which were grown on LB plate with 50 μ g/mL kanamycin overnight at 37 °C. On day two in the morning, one colony was picked and inoculated into 400 μ L LB medium with 25 g/mL chloramphenicol and was grown to OD 1.0 (measured in 200 μ L volume in 96-well plate by plate reader for absorbance at 600 nm) in a 5 mL culture tube in the shaker. The cells were then diluted 1000 folds into 2 mL fresh LB medium supplemented with $1.25 \times 10^{-3}\%$ of L-ara, and grew in a 15 mL culture tube with 250 rpm at 37 °C for 16 h. On day three, cells inducted in the last step were 100-fold diluted into each culture medium of the varied nutrient levels supplemented with the desired concentration of L-ara and antibiotics. Then, three technical replicates of 200 μ L culture mix for each culture medium of the varied nutrient levels were load onto a 96-well plate, which was immediately placed onto the plate-reader to start the measurement.

The experimental procedure for each biological replicate of the toggle switch induction was carried out as above, except for the strain being K-12 MG1655 Δ lacI, antibiotics being 50 μ g/mL kanamycin, and the inducer being 4 ng/mL aTc.

The experimental procedure for each biological replicate of the constitutive circuit induction was carried out as the induction of SA-circuit.

Dynamic Analysis Performed by Plate Reader. Synergy H1 Hybrid Reader from BioTek was used to perform the average fluorescence analysis. 200 μ L of culture was loaded into each well of the 96-well plate. M9 broth without cells was used as blank. LB broth without cells was used to set the low-scale of the fluorescence. The plate was incubated at 37 °C with orbital shaking at the frequency of 807 cpm (cycles per minute). The duration of the measurement was 18 h and the interval between each measurement was 30 min. Optical density (OD) of the culture was measured by absorbance at 600 nm; GFP was detected by excitation/emission at 485/515 nm.

Mathematical Model for the SA Circuit by Considering the Growth-Rate Regulation on Gene Production Rate. Here, we followed our previous work¹⁹ to model the dynamics of the circuit gene expression and cell density. For this work, the dependence of the production rate of the gene circuit on the growth rate of the host cell is considered, following the suggestion about the realistic description of growth effects.⁴⁴ The revised model follows is given by

$$\frac{\mathrm{d}[AraC]}{\mathrm{d}t} = f([AraC]) \cdot F(g) - d \cdot [AraC] - g \cdot [AraC],$$

$$\frac{\mathrm{d}N}{\mathrm{d}t} = g \cdot N$$

where $f = k_0 + k_1(S_a \cdot [AraC]^2)/(S_a \cdot [AraC]^2 + 1)$, k_0 and k_1 are is the basal production rate and the maximum L-arainduced production rate of AraC respectively, S_a describes how the production rate is regulated by the inducer L-ara, d and g are the degradation rate and dilution rate, respectively. [AraC] is the concentration of AraC, which is coexpressed with GFP and thus used interchangeably. N is the cell density, the growth rate $g = k_o(1 - N/N_{\text{max}})/([AraC]/J + 1)$, where *J* is defined as the overload parameter of the gene circuit to the growth rate. k_g is the maximal growth rate and N_{max} is the carrying capacity. Here we considered several functions of F(g) to fit the experimental data and to find the correct phenomenological dependence of the synthetic gene production rate on growth rate. The function F(g) represents the regulation of synthesis rate of AraC by the growth rate. We used F(g) = 1 to describe the scenario where the synthetic gene production rate is independent of growth rate, $F(g) = a \cdot g + b$ (linear), and F(g)= $(a \cdot g + b)/(c \cdot g + 1)$ (monotonic) to describe the scenario where the synthetic gene production rate monotonically increases with growth rate, and $F(g) = ((a \cdot g)^{n_1} + b)/((c \cdot g)^{n_2} + b)$ g^{n_2}) + 1) (nonmonotonic, with $n_1 < n_2$) to describe the scenario where the synthetic gene production rate nonmonotonically changes with growth rate. The best fitted parameters with this model, unless otherwise mentioned, are as follows: a = 0.0079 h, b = 1, $k_0 = 0.4488 \text{ a.u./h}$, $k_1 = 8.9770$ a.u./h, $S_a = 1$, d = 4.4885/h, $k_g = 0.9634/h$, J = 2.8066 a.u.; for the linear case, while for the monotonic case: a = 727.7 h, b =1, c = 277.5 h, $k_0 = 0.0289 a.u./h$, $k_1 = 0.5779 a.u./h$, $S_a = 1$, d = 0.5779 a.u./h0.2889/h, $k_g = 0.9065/h$, J = 8.1291 a.u.; and nonmonotonic case: a = 56.9874 h, b = 1, c = 2.5885 h, $n_1 = 0.5$, $n_2 = 2$, $k_0 = 0.5$ 0.0514 a.u./h, $k_1 = 1.0288$ a.u./h, $S_a = 1$, d = 0.5144/h, $k_{\sigma} =$ 1.2540/h, J = 2.1230 a.u.

Mathematical Model for the SA Circuit by Considering the Ribosome Allocation to the Host Cell Growth and Synthetic Gene Circuits. In order to understand the underlying molecular mechanism for the oscillatory dynamics, we also developed a model by explicitly considering the ribosome allocation for cell maintenance, growth feedback, and circuit gene. It was reported that the promoter activity in many conditions is approximately constant during about two cell cycles in midexponential growth phase, 45 where we found the overshoot. In addition, the ribosome is considered as a primary determinant of growth rate 46 and the major resource that is competed by synthetic gene circuit. 15,47 Thus, here we considered ribosome allocation as the major component in the model. The revised equation for the gene circuit follows

$$\frac{\mathrm{d}[AraC]}{\mathrm{d}t} = f([AraC]) \cdot R_{cf} - d \cdot [AraC] - g \cdot [AraC]$$

where R_{cf} is the relative ribosome allocated to the synthetic gene circuit, which depends on the cellular ribosome level and growth rate (see below).

The ribosome level is not a constant but heavily depends on the cell growth rate. It has been found that the *E. coli* cell tunes its ribosome level to be linearly correlated with growth rate. ^{21,48,49} Furthermore, at zero growth, the ribosome level in *E. coli* cells is maintained at a basal level, ^{31,48} which supports the normal physiology of cells with a constant protein production activity in the stationary phase for a very long time ⁵⁰ and could also support the gene expression in synthetic gene circuits. ¹⁹ In addition, the production of the ribosome is also regulated by its autocatalysis. ^{51,52} Here we incorporated these regulations into the mathematical model to represent the dynamic regulation of ribosome,

$$\frac{d[R]}{dt} = k_{r0} + k_{r1} \cdot H([R], g_0) - g \cdot [R] - d_r \cdot [R]$$

where we set $H([R], g_0) = g_0 \cdot [R]^n/([R]^n + K^n)$ to describe that the ribosome synthesis is linearly controlled by growth rate and also its autocatalysis. Here we used a Hill function to describe the autocatalysis of ribosomes. This is consistent with the experimental observation that ribosomal promoter activity increases with growth rate.⁴⁹ By solving this equation at zero growth $(g_0 = 0)$, we can get the basal level of ribosome as $R_{\min} = k_{r0}/d_r$.

Here, the ribosome is allocated into three classes for simplicity, including cell maintenance (R_0) , growth (R_g) and circuit gene production (R_C) . First, we assume that a constant amount of ribosome R_0 is allocated to cell normal maintenance with a high priority for translating the genes that are essential to the cell survival, including house-keeping genes. Then the rest of ribosome could be allocated to cell growth if the nutrient is sufficient or synthetic gene circuits according to their demands. The production of the exogenous genes can cause a metabolic burden to the host. 19 The growth rate without the metabolic burden is represented by $g_0 = k_g(1 - N/I)$ N_{max}). The ribosome working on growth is given by $R_g = (g/$ $k_{\nu}(R-R_0)$. The ribosome expression at zero growth rate (R_{min}) is able to maintain a steady state level of the gene expression. The amount of ribosome producing AraC at steady state is $(R_{\min} - R_0)$. Therefore, the fraction of ribosome available for gene production in respect to steady state of the circuit is represented by $R_{cf} = (R - R_g - R_0)/(R_{min} - R_0)$. The best fitted parameters with this model, unless otherwise mentioned, are as follows: $k_0 = 0.0335$ a.u./h, $k_1 = 0.6698$ a.u./ h, $S_a = 1.1453$, d = 0.3349/h, $k_a = 0.9945$ /h, J = 2.1919 a.u., k_{r0} = 0.0879 a.u./h, k_{r1} = 1.7581 a.u./h, K = 0.7988 a.u., d_r = 0.8790/h, n = 1 and $R_0 = 0.0599$ a.u.

Mathematical Model for the Toggle Switch. Following the model for the toggle switch in our previous work ^{19,34} and the above modeling framework for the SA circuit, we developed the following ODE model to describe the dynamics of LacI and TetR concentration ([*LacI*] and [*TetR*]) in the toggle switch,

$$\frac{\text{d}[LacI]}{\text{d}t} = f1([LacI], [TetR]) \cdot R_{cf} - d \cdot [LacI] - g \cdot [LacI],$$

$$\frac{\text{d}[TetR]}{\text{d}t} = f2([LacI], [TetR]) \cdot R_{cf} - d \cdot [TetR]$$

$$- g \cdot [TetR]$$

where
$$f1 = crl + \frac{1}{1.0 + \left[\frac{[TeR]}{k_l} \cdot \left(1.0 + \frac{aTc}{k_{atc}} \cdot \frac{k_t}{[TeR]}\right)^{-m}\right]^{nt}} \cdot (cil - crl),$$

$$f2 = crt + \frac{1}{1 + \left(\frac{[LacI]}{k_I}\right)^{nl}} \cdot (cit - crt)$$
. crl and cil are the produc-

tion rates of LacI when its promoter is repressed or induced, respectively. k_t is the TetR concentration that makes 50% of the maximum inhibition on LacI, and nt describes the ultrasensitivity of this inhibition. m is the Hill coefficient to describe the relationship between the active ratio of repressor TetR and the aTc inducer concentration. crt and cit are the production rates of TetR when its promoter is repressed or induced. k_l is the LacI concentration that makes 50% of the maximum inhibition on TetR, and nl describes the ultrasensitivity of this inhibition. d is the degradation rate constant, and the g is growth rate, which is represented by $g = k_{\sigma}(1 - N/$ N_{max})/(1 + ([LacI] + [TetR])/J). LacI is coexpressed with GFP, and thus was used interchangeably. R_{cf} can be calculated following the modeling framework in the above section for the SA circuit. The best fitted parameters with this model, unless otherwise mentioned, are as follows: crl = 0.1 a.u./h, cil = 4.25a.u./h, $k_t = 6$ a.u., $k_{atc} = 0.54$ ng/mL, m = 3, nt = 1.5, crt = 0.5a.u./h, cit = 4.25 a.u./h, $k_l = 8$ a.u., nl = 3.5, d = 0.1/h, J = 50a.u., $k_g = 1.2/h$, aTc = 4 ng/mL, $k_{r0} = 0.0879$ a.u./h, $k_{r1} =$ 1.7581 a.u./h, K = 0.7988 a.u., $d_r = 0.8790/h$, n = 1 and $R_0 = 0.8790/h$ 0.0599 a.u.

Parameter Fitting. For fitting of parameters to the experimental data, we used the Matlab function fminsearch, which minimizes the least-squares error between the model simulation results and the experimental data.

ASSOCIATED CONTENT

Supporting Information

The Supporting Information is available free of charge at https://pubs.acs.org/doi/10.1021/acssynbio.1c00041.

Mathematical proof on the monotonicity of the growth rate-dependent function on the circuit gene production rate; Figures S1–S5 (PDF)

AUTHOR INFORMATION

Corresponding Authors

Rong Zhang — School of Biological and Health Systems Engineering, Arizona State University, Tempe, Arizona 85281, United States; Email: rong_zhang@asu.edu

Xiao-Jun Tian — School of Biological and Health Systems
Engineering, Arizona State University, Tempe, Arizona
85281, United States; orcid.org/0000-0002-5601-2057;
Email: xiaojun.tian@asu.edu

Authors

Juan Melendez-Alvarez — School of Biological and Health Systems Engineering, Arizona State University, Tempe, Arizona 85281, United States

Changhan He — School of Mathematical and Statistical Sciences, Arizona State University, Tempe, Arizona 85281, United States

Yang Kuang — School of Mathematical and Statistical Sciences, Arizona State University, Tempe, Arizona 85281, United States

Complete contact information is available at: https://pubs.acs.org/10.1021/acssynbio.1c00041

Author Contributions

X.-J.T. and R.Z. conceived the study. X.-J.T., R.Z., and Y.K. designed the study. R.Z. performed experiments. J.M.-A., C.H., Y.K., and X.-J.T. performed modeling analysis. R.Z., J.M.-A., and X.-J.T. analyzed the experimental data. J.M.-A. and X.-J.T. wrote the manuscript. C.H., R.Z., and Y.K. edited the manuscript.

Notes

The authors declare no competing financial interest.

ACKNOWLEDGMENTS

This project was supported by the ASU School of Biological and Health Systems Engineering and NSF grants (EF-1921412 to X.-J.T.; DEB-1930728 to Y.K.), NIH grant (5R01GM131405 to Y.K.). J.M.-A. was also supported by the Arizona State University Dean's Fellowship.

REFERENCES

- (1) Lu, T. K., Khalil, A. S., and Collins, J. J. (2009) Next-generation synthetic gene networks. *Nat. Biotechnol.* 27, 1139–1150.
- (2) Purnick, P. E., and Weiss, R. (2009) The second wave of synthetic biology: from modules to systems. *Nat. Rev. Mol. Cell Biol.* 10, 410–22.
- (3) Brophy, J. A., and Voigt, C. A. (2014) Principles of genetic circuit design. *Nat. Methods* 11, 508–20.
- (4) Sprinzak, D., and Elowitz, M. B. (2005) Reconstruction of genetic circuits. *Nature* 438, 443–8.
- (5) Del Vecchio, D. (2015) Modularity, context-dependence, and insulation in engineered biological circuits. *Trends Biotechnol.* 33, 111–9.
- (6) Yeung, E., Dy, A. J., Martin, K. B., Ng, A. H., Del Vecchio, D., Beck, J. L., Collins, J. J., and Murray, R. M. (2017) Biophysical Constraints Arising from Compositional Context in Synthetic Gene Networks. *Cell Syst 5*, 11–24.
- (7) Liao, C., Blanchard, A. E., and Lu, T. (2017) An integrative circuit-host modelling framework for predicting synthetic gene network behaviours. *Nat. Microbiol* 2, 1658–1666.
- (8) Boo, A., Ellis, T., and Stan, G.-B. (2019) Host-aware synthetic biology. Curr. Opin Syst. Biol. 14, 66–72.
- (9) Sanchez-Osorio, I., Hernandez-Martinez, C. A., and Martinez-Antonio, A. (2020) Quantitative modeling of the interplay between synthetic gene circuits and host physiology: experiments, results, and prospects. *Curr. Opin. Microbiol.* 55, 48–56.
- (10) Zhang, C., Tsoi, R., and You, L. (2016) Addressing biological uncertainties in engineering gene circuits. *Integr Biol.* (*Camb*) 8, 456–64.
- (11) Charlebois, D. A., Hauser, K., Marshall, S., and Balázsi, G. (2018) Multiscale effects of heating and cooling on genes and gene networks. *Proc. Natl. Acad. Sci. U. S. A. 115*, E10797—e10806.
- (12) Ceroni, F., Algar, R., Stan, G. B., and Ellis, T. (2015) Quantifying cellular capacity identifies gene expression designs with reduced burden. *Nat. Methods* 12, 415–8.
- (13) Ceroni, F., Boo, A., Furini, S., Gorochowski, T. E., Borkowski, O., Ladak, Y. N., Awan, A. R., Gilbert, C., Stan, G. B., and Ellis, T. (2018) Burden-driven feedback control of gene expression. *Nat. Methods* 15, 387–393.
- (14) Borkowski, O., Ceroni, F., Stan, G. B., and Ellis, T. (2016) Overloaded and stressed: whole-cell considerations for bacterial synthetic biology. *Curr. Opin. Microbiol.* 33, 123–130.
- (15) Gyorgy, A., Jimenez, J. I., Yazbek, J., Huang, H. H., Chung, H., Weiss, R., and Del Vecchio, D. (2015) Isocost Lines Describe the Cellular Economy of Genetic Circuits. *Biophys. J.* 109, 639–46.
- (16) Qian, Y., Huang, H. H., Jimenez, J. I., and Del Vecchio, D. (2017) Resource Competition Shapes the Response of Genetic Circuits. ACS Synth. Biol. 6, 1263–1272.

- (17) Blanchard, A. E., Liao, C., and Lu, T. (2018) Circuit-Host Coupling Induces Multifaceted Behavioral Modulations of a Gene Switch. *Biophys. J.* 114, 737–746.
- (18) Nikolados, E. M., Weisse, A. Y., Ceroni, F., and Oyarzun, D. A. (2019) Growth Defects and Loss-of-Function in Synthetic Gene Circuits. *ACS Synth. Biol.* 8, 1231–1240.
- (19) Zhang, R., Li, J., Melendez-Alvarez, J., Chen, X., Sochor, P., Goetz, H., Zhang, Q., Ding, T., Wang, X., and Tian, X. J. (2020) Topology-dependent interference of synthetic gene circuit function by growth feedback. *Nat. Chem. Biol.* 16, 695–701.
- (20) Zhang, R., Goetz, H., Melendez-Alvarez, J., Li, J., Ding, T., Wang, X., and Tian, X.-J. (2021) Winner-Takes-All Resource Competition Redirects Cascading Cell Fate Transitions. *Nat. Commun.*, DOI: 10.1038/s41467-021-21125-3.
- (21) Scott, M., Gunderson, C. W., Mateescu, E. M., Zhang, Z., and Hwa, T. (2010) Interdependence of cell growth and gene expression: origins and consequences. *Science* 330, 1099–102.
- (22) Deris, J. B., Kim, M., Zhang, Z., Okano, H., Hermsen, R., Groisman, A., and Hwa, T. (2013) The innate growth bistability and fitness landscapes of antibiotic-resistant bacteria. *Science* 342, 1237435.
- (23) Klumpp, S., and Hwa, T. (2014) Bacterial growth: global effects on gene expression, growth feedback and proteome partition. *Curr. Opin. Biotechnol.* 28, 96–102.
- (24) Tan, C., Marguet, P., and You, L. (2009) Emergent bistability by a growth-modulating positive feedback circuit. *Nat. Chem. Biol. 5*, 842–8.
- (25) Sickle, J. J., Ni, C., Shen, D., Wang, Z., Jin, M., and Lu, T. (2020) Integrative Circuit-Host Modeling of a Genetic Switch in Varying Environments. *Sci. Rep.* 10, 8383.
- (26) Becskei, A., Séraphin, B., and Serrano, L. (2001) Positive feedback in eukaryotic gene networks: cell differentiation by graded to binary response conversion. *Embo j 20*, 2528–35.
- (27) Stevenson, K., McVey, A. F., Clark, I. B. N., Swain, P. S., and Pilizota, T. (2016) General calibration of microbial growth in microplate readers. *Sci. Rep. 6*, 38828.
- (28) Dai, X., and Zhu, M. (2020) Coupling of Ribosome Synthesis and Translational Capacity with Cell Growth. *Trends Biochem. Sci.* 45, 681.
- (29) Bren, A., Hart, Y., Dekel, E., Koster, D., and Alon, U. (2013) The last generation of bacterial growth in limiting nutrient. *BMC Syst. Biol.* 7, 27.
- (30) Iyer, S., Le, D., Park, B. R., and Kim, M. (2018) Distinct mechanisms coordinate transcription and translation under carbon and nitrogen starvation in Escherichia coli. *Nat. Microbiol* 3, 741–748.
- (31) Li, S. H., Li, Z., Park, J. O., King, C. G., Rabinowitz, J. D., Wingreen, N. S., and Gitai, Z. (2018) Escherichia coli translation strategies differ across carbon, nitrogen and phosphorus limitation conditions. *Nat. Microbiol* 3, 939–947.
- (32) Balazsi, G., van Oudenaarden, A., and Collins, J. J. (2011) Cellular decision making and biological noise: from microbes to mammals. *Cell* 144, 910–25.
- (33) Ray, J. C., Wickersheim, M. L., Jalihal, A. P., Adeshina, Y. O., Cooper, T. F., and Balázsi, G. (2016) Cellular Growth Arrest and Persistence from Enzyme Saturation. *PLoS Comput. Biol.* 12, e1004825.
- (34) Menn, D., Sochor, P., Goetz, H., Tian, X. J., and Wang, X. (2019) Intracellular Noise Level Determines Ratio Control Strategy Confined by Speed-Accuracy Trade-off. ACS Synth. Biol. 8, 1352—1360.
- (35) Kheir Gouda, M., Manhart, M., and Balazsi, G. (2019) Evolutionary regain of lost gene circuit function. *Proc. Natl. Acad. Sci. U. S. A. 116*, 25162–25171.
- (36) Potrykus, K., Murphy, H., Philippe, N., and Cashel, M. (2011) ppGpp is the major source of growth rate control in E. coli. *Environ. Microbiol.* 13, 563–575.
- (37) Zhu, M., and Dai, X. (2019) Growth suppression by altered (p)ppGpp levels results from non-optimal resource allocation in Escherichia coli. *Nucleic Acids Res.* 47, 4684–4693.

- (38) Lemke, J. J., Sanchez-Vazquez, P., Burgos, H. L., Hedberg, G., Ross, W., and Gourse, R. L. (2011) Direct regulation of Escherichia coli ribosomal protein promoters by the transcription factors ppGpp and DksA. *Proc. Natl. Acad. Sci. U. S. A. 108*, 5712–7.
- (39) Hauryliuk, V., Atkinson, G. C., Murakami, K. S., Tenson, T., and Gerdes, K. (2015) Recent functional insights into the role of (p)ppGpp in bacterial physiology. *Nat. Rev. Microbiol.* 13, 298–309.
- (40) Traxler, M. F., Summers, S. M., Nguyen, H. T., Zacharia, V. M., Hightower, G. A., Smith, J. T., and Conway, T. (2008) The global, ppGpp-mediated stringent response to amino acid starvation in Escherichia coli. *Mol. Microbiol.* 68, 1128–48.
- (41) Shachrai, I., Zaslaver, A., Alon, U., and Dekel, E. (2010) Cost of unneeded proteins in E. coli is reduced after several generations in exponential growth. *Mol. Cell* 38, 758–67.
- (42) Scott, M., Klumpp, S., Mateescu, E. M., and Hwa, T. (2014) Emergence of robust growth laws from optimal regulation of ribosome synthesis. *Mol. Syst. Biol.* 10, 747.
- (43) Shyp, V., Tankov, S., Ermakov, A., Kudrin, P., English, B. P., Ehrenberg, M., Tenson, T., Elf, J., and Hauryliuk, V. (2012) Positive allosteric feedback regulation of the stringent response enzyme RelA by its product. *EMBO Rep. 13*, 835–9.
- (44) Hintsche, M., and Klumpp, S. (2013) Dilution and the theoretical description of growth-rate dependent gene expression. *J. Biol. Eng.* 7, 22.
- (45) Setty, Y., Mayo, A. E., Surette, M. G., and Alon, U. (2003) Detailed map of a cis-regulatory input function. *Proc. Natl. Acad. Sci. U. S. A. 100*, 7702–7707.
- (46) Belliveau, N. M., Chure, G. D., Hueschen, C. L., Garcia, H. G., Kondev, J., Fisher, D. S., Theriot, J. A., and Phillips, R. (2020) Fundamental limits on the rate of bacterial growth. *bioRxiv*, Oct 18, 2020. DOI: 10.1101/2020.10.18.344382.
- (47) Vind, J., Sørensen, M. A., Rasmussen, M. D., and Pedersen, S. (1993) Synthesis of proteins in Escherichia coli is limited by the concentration of free ribosomes. Expression from reporter genes does not always reflect functional mRNA levels. *J. Mol. Biol.* 231, 678–88.
- (48) Dai, X., Zhu, M., Warren, M., Balakrishnan, R., Patsalo, V., Okano, H., Williamson, J. R., Fredrick, K., Wang, Y. P., and Hwa, T. (2017) Reduction of translating ribosomes enables Escherichia coli to maintain elongation rates during slow growth. *Nat. Microbiol* 2, 16231
- (49) Zaslaver, A., Kaplan, S., Bren, A., Jinich, A., Mayo, A., Dekel, E., Alon, U., and Itzkovitz, S. (2009) Invariant Distribution of Promoter Activities in Escherichia coli. *PLoS Comput. Biol.* 5, e1000545.
- (50) Gefen, O., Fridman, O., Ronin, I., and Balaban, N. Q. (2014) Direct observation of single stationary-phase bacteria reveals a surprisingly long period of constant protein production activity. *Proc. Natl. Acad. Sci. U. S. A. 111*, 556–61.
- (51) Reuveni, S., Ehrenberg, M., and Paulsson, J. (2017) Ribosomes are optimized for autocatalytic production. *Nature* 547, 293–297.
- (52) Chandra, F., and Del Vecchio, D. (2016) The Effects of Ribosome Autocatalysis and Negative Feedback in Resource Competition. *bioRxiv*, Mar 4, 2016. DOI: 10.1101/042127.